THE JOURNAL OF PHYSICAL CHEMISTRY Letters

pubs.acs.org/JPCL Letter

Rotational and Vibrational Excitations of a Single Water Molecule by Inelastic Electron Tunneling Spectroscopy

Jianmei Li, Qiuhao Xu, Lihuan Sun, Jiyu Xu, Dong Hao, Xiangqian Tang, Xinyan Shan, Sheng Meng,* and Xinghua Lu*

Cite This: J. Phys. Chem. Lett. 2020, 11, 1650−1655 Read Online

ACCESS | Metrics & More | Article Recommendations | Supporting Information

ABSTRACT: Two low-energy excitations of a single water molecule are observed via inelastic electron tunneling spectroscopy, where a significant enhancement is achieved by attaching the molecule to the tip apex in a scanning tunneling microscope. Density functional theory simulations and quantum mechanical calculations of an asymmetric top are carried out to reveal the origin of both excitations. Variations in tunneling junction separation give rise to the quantum confinement effect on the quantum state of a water molecule in the tunneling junction. Our results demonstrate a potential method for measuring the dynamic behavior of a single molecule confined in a tunneling junction, where the molecule−substrate interaction can be purposely tuned.

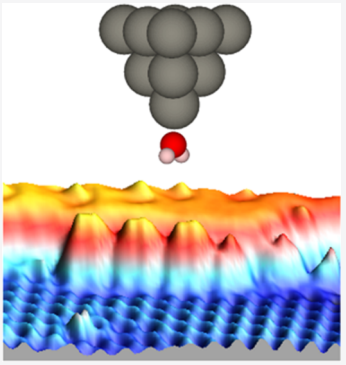

The atomic structure of water and its dynamic behavior play an indispensable role in a large class of processes in physics, chemistry, and biology as well as in technology developments. For example, water molecules confined in one-dimensional carbon nanotubes exhibit abnormally large permeability,[1] and those in a biological nanopore can mediate the recognition of DNA sequences.[2] The structure, stability, functionality, and reactivity of biomolecules and H-bonded materials[1,3,4] are closely related to the rotational and vibrational behavior of water molecules at the nanoscale.

Optical spectroscopy and diffraction technologies[5−8] have been employed widely in probing the rotational and vibrational modes of water molecules in various environments. High spatial resolutions up to the single-molecule scale, however, are strongly desired to fully understand the behavior of water molecules in the confined environments such as on a reconstructed atomic surface or in a nanocavity. Scanning probe microscopies, including scanning tunneling microscopy (STM) and atomic force microscopy (AFM), are unique in imaging surfaces with ultimate atomic resolution. High-resolution topographic images of water clusters on surfaces have been obtained, revealing characteristics and novel phenomena in hydrogen bond networks.[9−11] In particular, inelastic electron tunneling spectroscopy (IETS) enables single-bond vibrational sensitivity with subangstrom spatial resolution.[12−14] Bending and stretching modes with energies of >100 meV have been detected for individual water molecules.[15] With a Cl-functionalized STM tip, nuclear quantum effects on H-bonding interaction of water molecules have been revealed by enhanced IETS. Strong tip height-dependent IETS peaks of a single molecule may reveal a variety of physical processes and mechanisms. IETS of CO on the Cu(111) surface, for example, is used to monitor the formation of a metal nanocontact.[16] Nonetheless, probing the rotational and vibrational modes of a single water molecule that are typically below 100 meV in energy is still extremely challenging.

Here we report a study in which we probed low-energy excitations of a single water molecule through tip-enhanced IETS. Two low-energy inelastic peaks are observed when the water molecule is attached to the STM tip apex. The energy of the modes is sensitive to the tunneling junction distance, indicating the influence of the substrate on the structure of the molecule at the tip apex. Density functional theory (DFT) simulation and theoretical calculation are carried out to identify the corresponding vibrational and rotational states, which also manifest the dynamic behavior of the single water molecule under different interaction strengths with the substrate as the tip−substrate distance changes.

The experiments were performed with a home-built scanning tunneling microscope operating at 12 K and with a base pressure of 10^{-11} Torr. The Cu(100) surface was cleaned by cycles of Ar^+ sputtering and annealing at 800 K. Atomic-thickness insulating Cu_2N islands were grown by sputtering the

Received: January 9, 2020
Accepted: February 10, 2020
Published: February 10, 2020

https://dx.doi.org/10.1021/acs.jpclett.0c00093
J. Phys. Chem. Lett. 2020, 11, 1650−1655

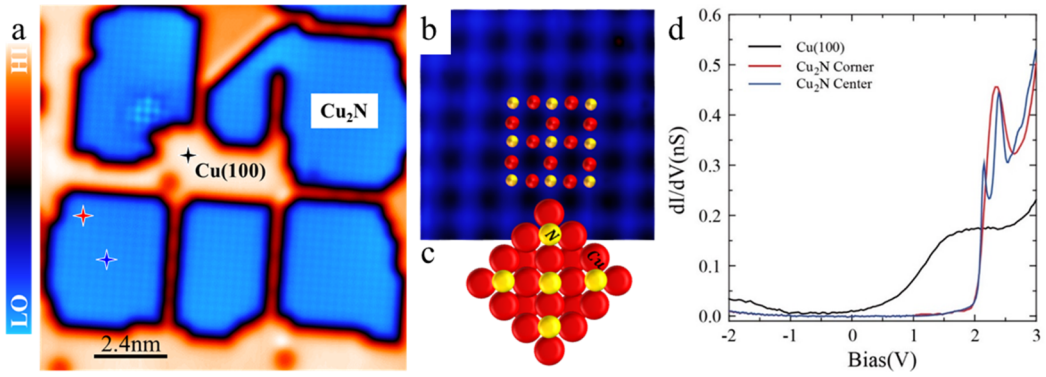

Figure 1. Cu_2N islands on a Cu(100) surface. (a) STM topography of Cu_2N islands as grown on a Cu(100) surface. Image size: 12 nm × 12 nm; imaging condition at V = 1 V and I = 0.5 nA. (b and c) Atom-resolved topographic image and atomic geometry of Cu_2N, respectively. Cu atoms and N atoms are shown as red and yellow spheres, respectively. (d) Electron tunneling spectroscopy data taken on Cu_2N islands and on a bare Cu(100) surface, at positions marked in panel a.

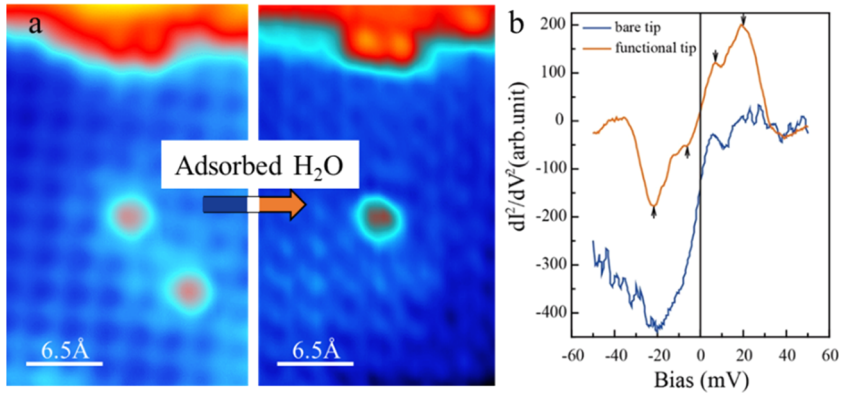

Figure 2. Manipulation of a single water molecule onto the STM tip. (a) STM topography of a Cu_2N island with two adsorbed water molecules in middle of the island (left), acquired with the bare W tip. STM topography of the same area after manipulating one of the water molecules to the tip (right). The manipulation is done by a voltage pulse. Images are acquired with at 50 mV and 0.1 nA. (b) d^2I/dV^2 spectra acquired over the center of a water molecule with the bare W tip and on a Cu_2N surface with a water-functionalized tip after manipulation.

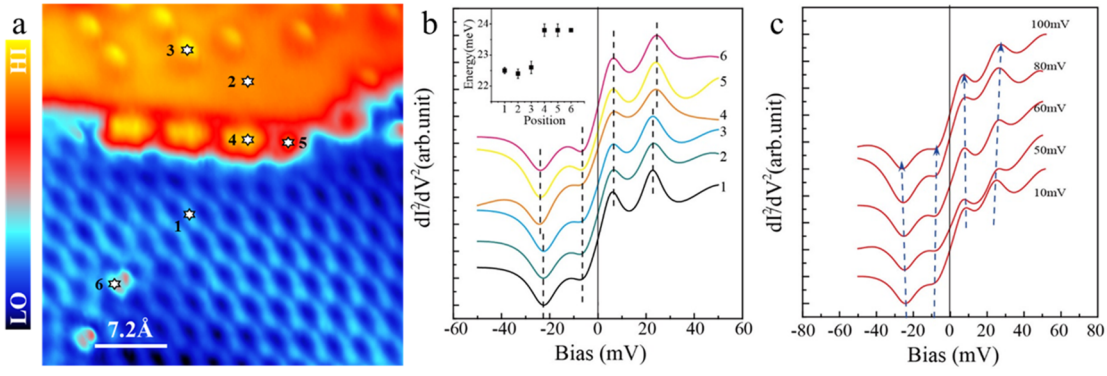

Figure 3. IETS of a single water molecule attached to the STM tip apex. (a) STM topography of the surface with a single water molecule attached to the STM tip. (b) d^2I/dV^2 spectra taken at different locations on the surface, as marked in panel a. Tunneling gap set by V = 50 mV and I = 0.5 nA. The inset shows the variation in the peak energy of IETS. (c) Normalized d^2I/dV^2 spectra taken over the center of the N atom on the Cu_2N substrate at different tip−substrate distances. The blue dotted lines highlight the shifts of peak positions.

Cu crystal surface with nitrogen ions N^+ at a vacuum pressure of 10^{-5} Torr and subsequent annealing at 500 K for 100 min. Water molecules are dosed onto the sample surface with a partial pressure (ΔP) of $\sim 10^{-11}$ Torr for 60 s while the crystal was kept in the cryogenic STM stage. The W tip was electrochemically etched and annealed in vacuum to remove the oxide on the tip surface. Tunneling spectroscopies were performed with a lock-in amplifier by applying a sinusoidal modulation (264 Hz, 8 mV in amplitude) in the sample bias and measuring the corresponding modulation in the tunneling current with feedback off. The spectroscopies were averages of three scans with sample bias range from −100 to 100 mV.

Figure 1a shows a topographic image of the sample surface with multiple Cu_2N islands that appear lower than the Cu surface due to the lack of density of states. The atomic structure of the Cu_2N islands is shown in panels b and c of

https://dx.doi.org/10.1021/acs.jpclett.0c00093
J. Phys. Chem. Lett. 2020, 11, 1650−1655

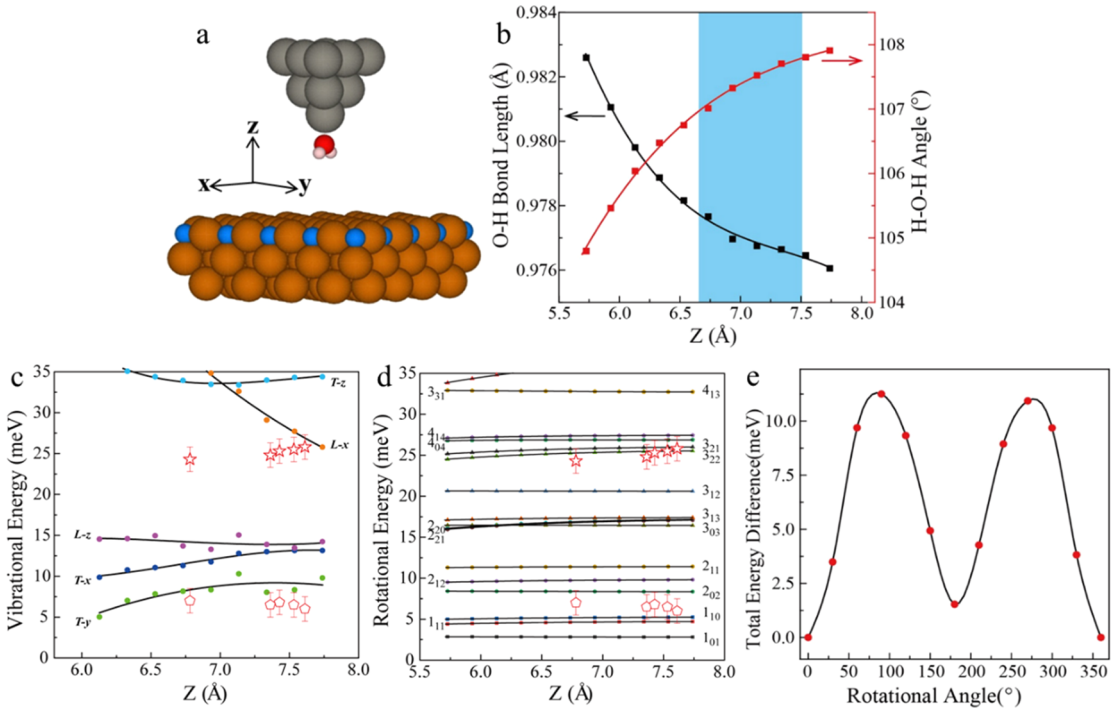

Figure 4. DFT simulation of the water molecule confined between the STM tip and the $Cu_2N/Cu(100)$ substrate. (a) Theoretical setup of a single water molecule attached to the tip. (b) Optimized geometry parameters of the water molecule as a function of tip height. Black and red lines represent the O−H bond length and H−O−H angle of the water molecule, respectively. The blue area indicates the approximate range probed by the experiment. (c) Calculated vibrational modes of the water molecule as a function of the tip height. (d) Calculated excitation energy for the rotational eigen modes. For panels c and d, within the energy range of 0−35 meV. The experimental data are also shown. (e) Total energy difference of a water molecule rotating around the z axis, with the tip−substrate distance set at 6.5 Å.

Figure 1. The distance between two adjacent N atoms is 3.7 Å, slightly larger than the lattice constant of the Cu(100) surface. This lattice mismatch limits the size of Cu_2N islands to several nanometers. The protrusions in the topographic image correspond to one-half of the 4-fold symmetric hollow sites of four adjacent Cu atoms on the Cu(100) surface, and the nitrogen (N) atoms adsorb on the other half of the hollow sites forming incommensurate $c(2 \times 2)$ lattice.[17,18] The overall coverage of Cu_2N islands in our experiment is in the range of 50−60% (see the Supporting Information).

Figure 1d shows the scanning tunneling spectroscopy (STS) data measured on the Cu_2N island and the bare Cu(100) surface. The local density of state (LDOS) of Cu_2N exhibits a band gap of >4 eV, illustrating electronic decoupling from the conducting metallic substrate underneath. The conduction band edge of Cu_2N is ∼2 eV above the Fermi level, and the LDOS in the energy range of 2−2.5 eV varies when taken on different regions of the Cu_2N island and on islands of different sizes due to the quantum confinement effect.[19]

After deposition, individual water molecules were observed on the Cu_2N island while water clusters were observed at the edges of the islands and on the Cu(100) surface. Most water molecules adsorbed onto the bare Cu surface, indicating the hydrophobic nature of the Cu_2N surface. The water molecule can be manipulated to the tip end by applying a voltage pulse (1 V in amplitude, 1 s in duration) in the sample bias. Figure 2a shows the topography before and after the manipulation process. We note that the spatial resolution in topography is apparently increased with a water molecule attached to the STM tip, which is a common practice in STM studies of single molecules.[20−22] With closer scanning conditions, Figure 3a shows the topographic image of water molecules adsorbed on a Cu_2N surface exhibiting a double-lobe structure similar to that as imaged on a NaCl film.[23] In addition, the imaged lattice structure of the Cu_2N surface changes from square to orthorhombic, due to the modification in LDOS of the STM tip with the water molecule attached at its apex.[24]

Detecting low-energy excitation mode in water molecules by IETS with a normal STM tip is difficult due to the strong electronic coupling to the substrate. Significant variation in IETS, however, is observed after the manipulation of the water molecule onto the tip apex. Two antisymmetric IETS peaks with energies of ∼24.5 meV and ∼6.5 meV are clearly observed via spectroscopy acquired with the water-functionalized STM tip, as shown in Figure 2b.

The IETS peaks originate from the water molecule attached to the STM tip and have a slight dependence on the surface location where the d^2I/dV^2 spectra are measured. Figure 3b shows IETS data recorded on various surface locations as marked in Figure 3a. The energy of the IETS peak around 7 meV remains the same across the surface, while the energy of the 25 meV peak shows a variation of a few millielectronvolts. The energy of the peak in IETS taken on water molecules absorbed on Cu_2N, both in the middle and at the edge of the island, is slightly higher than that taken on other locations (values shown in the inset of Figure 3b). Further detailed measurements show no variation in peak energy in IETS taken across the Cu_2N island, despite the apparent changes in the substrate LDOS (see the Supporting Information).

To investigate the effect of molecule−substrate interaction on the observed IETS peaks, we varied the tunneling gap distance by increasing the sample biases from 10 to 100 mV

https://dx.doi.org/10.1021/acs.jpclett.0c00093
J. Phys. Chem. Lett. 2020, 11, 1650−1655

while keep the tunneling current at 100 pA. The corresponding tunneling gap distance changes by approximately 0.8 Å through the measurements (see the Supporting Information). Energies of both peaks changed accordingly, from 24.3 to 25.8 meV and from 7 to 6 meV, for the high- and low-energy peaks, respectively.

The energies of the two observed IETS peaks are within the range of both rotational and vibrational modes of water molecules. To reveal the nature of both excited water modes, we performed DFT calculations with the VASP package. van der Waals interactions have been included by choosing the OptB88-vdw exchange-correlation functional.[25] Projector-augmented wave pseudopotentials[26] and an energy cutoff of 520 eV were used. The simulation box was 14.51 Å × 14.51 Å × 20 Å, and the *k*-point sampling is 3 × 3 × 1. A Cu_2N layer was used to represent the substrate, and the STM tip was simulated with 10 tungsten atoms. The apex of the tip was located above one of the nitrogen atoms in the substrate. The tungsten atom at the apex is relaxed, while all other atoms are fixed in all calculations. Before structure optimization, the water molecule was set to two different configurations. In one configuration, the molecular plane was set parallel to the substrate. In the other configuration, one of the OH bonds was set perpendicular to the substrate. Both initial configurations resulted in the same final water structure after relaxation, which ensured the most stable state for further analysis. In the final stable configuration, the oxygen atom of the water molecule bonds with the atom at the tip apex, and the dipole moment of molecule is nearly parallel to the *z* axis, as shown in Figure 4a.

Simulations were carried out by varying the tip−substrate distance from 5.7 to 7.7 Å. At each value of the tip−substrate separation, the molecular configuration of water was derived from the equilibrium state of the molecule, and all nine vibrational modes of the water molecule are calculated (see the Supporting Information). According to the DFT calculations, the O−H bond length decreases from 0.983 to 0.976 Å and the H−O−H angle increases from 104.8° to 107.9° when the tip−substrate separation increases from 5.7 to 7.7 Å as shown Figure 4b. The approximate range probed by the STM experiment is marked by the blue region. Figure 4c shows the vibrational modes that are within the energy range of 0−35 meV. The energies of experimentally measured IETS peaks are shown, as well. The low-energy peak is close to the *T-y* mode, and the high-energy mode is close to the *L-x* mode. Assigning the 25 meV peak to the *L-x* mode, however, encounters difficulty in that they do not change in the same direction when the tip−substrate distance changes, nor do they vary with similar sensitivity.

We notice that the water molecule also possesses rotational freedom when bonded to the apex atom of the tip. Rotational modes are then derived from the atomic configuration of the water molecule under various tip−substrate distances. The calculation is carried out following a standard quantum mechanical computational procedure,[5,27−30] where the excitation energies from the ground state to the rotational states are obtained (see the Supporting Information). The results are shown in Figure 4d, where the rotational modes within 35 meV in energy are plotted as a function of the tip−substrate distance. The mode energy increases slightly as the tip height increases. The 25 meV IETS peak matches best with rotational states 3_{21} and 3_{22} when excited from ground state 0_{00}. Quantum state J_{KaKc} is characterized by the total rotational angular momentum (J) and two projected momenta (Ka and Kc). For rotational states 3_{21} and 3_{22}, total angular momentum J is not along the symmetric axis of the water molecule. This is possible if we consider the reality that the water molecule may not be settled in a fully symmetric configuration as shown in the calculations. Experimentally, a tilted water molecule is plausible, as a symmetric water molecule would likely give the topographs a double-tip effect. Our experimentally measured topographs are clearly free of such artifacts, ruling out this possibility.

To further validate the assignment of the rotational modes, we calculated the energy barrier for water rotation along the *z* axis. Figure 4e shows the potential energy as the water molecule rotates around the *z* axis. The total energy difference is <11 meV, indicating that the water molecule in the rotational state with an energy around 25 meV is feasible. The IETS peak at 6 meV, for the same reason, cannot be assigned to the rotational mode by considering this rotational energy barrier. The decrease in the energy of this 6 meV mode as the tip−substrate distance increases provides further evidence that it is a vibrational mode. This is why only two modes are observed in the IETS spectra, partly due to the resolution of the measurements and the selection rule of excitation by tunneling electrons that deserves further investigations.

We also considered the effects of the electric field because there was a bias voltage applied in the tunneling junction during the experiment. An electric field of $\leq 10^9$ V/m has been applied along the *z* axis in the simulation, and the water molecule is relaxed to its ground state. No significant change in energy has been derived in either rotational mode (see the Supporting Information). Previous studies revealed absorption bands at 88 cm^{-1} (10.9 meV) and 158 cm^{-1} (19.6 meV) for water molecules confined within a nanocavity with the electric field perpendicular to the dipole moment of water molecules,[7,31] and the two resonance peaks strictly depend on the direction of the electric field. The inconsistency may come from the difference in environment or excitation method. For water molecules trapped in a nanocavity with a high-order symmetry, they behave more like a rotator with three rotational axes. When the water molecule is attached to the STM tip, the rotational freedom is restricted and only some of the rotational quantum states can be excited. The selection rule for optical excitation in optical absorption measurements is also different from that for excitation by tunneling electrons in STM experiments[14] and the rotational transition in inelastic neutron scattering (INS) spectra.[5]

In summary, two low-energy excitations of a single water molecule have been detected in inelastic electron tunneling spectroscopy by attaching the molecule to the STM tip. With a change in the tip−substrate distance, variations in the energy of the excitations are measured. Combined experimental data and theoretical calculation reveal that the low-energy excitation around 6 meV is related to the vibration of the molecule and the high-energy peak around 25 meV is very possibly due to the excitation of a rotational quantum state. The results demonstrate an enhancement method in detecting low-energy excitations of a single molecule confined in the STM tunneling junction, where the dynamic behavior of the molecule can be further tuned by the tip−substrate distance.

■ ASSOCIATED CONTENT

Supporting Information

The Supporting Information is available free of charge at https://pubs.acs.org/doi/10.1021/acs.jpclett.0c00093.

https://dx.doi.org/10.1021/acs.jpclett.0c00093
J. Phys. Chem. Lett. 2020, 11, 1650−1655

Large scale STM topography of Cu_2N islands, site dependence of the IETS spectra, vibrational modes of the water molecule determined by DFT simulation, electric field effect determined by DFT simulation and quantum mechanics calculation, tip height calculation, quantum mechanical calculation of rotational modes of a single water molecule, and energy diagram of rotational states of the water molecule (PDF)

AUTHOR INFORMATION

Corresponding Authors

Sheng Meng − *Beijing National Laboratory for Condensed Matter Physics, Institute of Physics, Chinese Academy of Sciences, Beijing 100190, China; School of Physical Sciences, University of Chinese Academy of Sciences, Beijing 100190, China; Songshan Lake Laboratory for Materials Science, Dongguan 523000, China;* orcid.org/0000-0002-1553-1432; Phone: +861082649396; Email: smeng@iphy.ac.cn

Xinghua Lu − *Beijing National Laboratory for Condensed Matter Physics, Institute of Physics, Chinese Academy of Sciences, Beijing 100190, China; School of Physical Sciences, University of Chinese Academy of Sciences, Beijing 100190, China; Songshan Lake Laboratory for Materials Science, Dongguan 523000, China; Center for Excellence in Topological Quantum Computation, Beijing 100190, China;* orcid.org/0000-0003-4228-0592; Phone: +861082648043; Email: xhlu@iphy.ac.cn

Authors

Jianmei Li − *Beijing National Laboratory for Condensed Matter Physics, Institute of Physics, Chinese Academy of Sciences, Beijing 100190, China; School of Physical Sciences, University of Chinese Academy of Sciences, Beijing 100190, China;* orcid.org/0000-0002-5529-5251

Qiuhao Xu − *Beijing National Laboratory for Condensed Matter Physics, Institute of Physics, Chinese Academy of Sciences, Beijing 100190, China; School of Physical Sciences, University of Chinese Academy of Sciences, Beijing 100190, China*

Lihuan Sun − *Beijing National Laboratory for Condensed Matter Physics, Institute of Physics, Chinese Academy of Sciences, Beijing 100190, China; School of Physical Sciences, University of Chinese Academy of Sciences, Beijing 100190, China;* orcid.org/0000-0002-4259-3313

Jiyu Xu − *Beijing National Laboratory for Condensed Matter Physics, Institute of Physics, Chinese Academy of Sciences, Beijing 100190, China; School of Physical Sciences, University of Chinese Academy of Sciences, Beijing 100190, China;* orcid.org/0000-0002-2628-5492

Dong Hao − *Beijing National Laboratory for Condensed Matter Physics, Institute of Physics, Chinese Academy of Sciences, Beijing 100190, China; School of Physical Sciences, University of Chinese Academy of Sciences, Beijing 100190, China*

Xiangqian Tang − *Beijing National Laboratory for Condensed Matter Physics, Institute of Physics, Chinese Academy of Sciences, Beijing 100190, China; School of Physical Sciences, University of Chinese Academy of Sciences, Beijing 100190, China*

Xinyan Shan − *Beijing National Laboratory for Condensed Matter Physics, Institute of Physics, Chinese Academy of Sciences, Beijing 100190, China*

Complete contact information is available at: https://pubs.acs.org/10.1021/acs.jpclett.0c00093

Notes

The authors declare no competing financial interest.

ACKNOWLEDGMENTS

Supported by the National Natural Science Foundation of China under Grants 11774395, 11774396 and 91753136, the Beijing Natural Science Foundation under Grant 4181003, the Ministry of Science and Technology of China under Grand No. 2016YFA0300902, and the Strategic Priority Research Program (B) of the Chinese Academy of Sciences under Grants XDB30201000 and XDB28000000.

REFERENCES

(1) Lee, B.; Baek, Y.; Lee, M.; Jeong, D. H.; Lee, H. H.; Yoon, J.; Kim, Y. H. A carbon nanotube wall membrane for water treatment. *Nat. Commun.* **2015**, *6*, 7109.

(2) Bhattacharya, S.; Yoo, J.; Aksimentiev, A. Water Mediates Recognition of DNA Sequence via Ionic Current Blockade in a Biological Nanopore. *ACS Nano* **2016**, *10* (4), 4644−51.

(3) Guo, Y.; Ding, Z.; Sun, L.; Li, J.; Meng, S.; Lu, X. Inducing Transient Charge State of a Single Water Cluster on Cu(111) Surface. *ACS Nano* **2016**, *10* (4), 4489−95.

(4) Dong, A.; Yan, L.; Sun, L.; Yan, S.; Shan, X.; Guo, Y.; Meng, S.; Lu, X. Identifying Few-Molecule Water Clusters with High Precision on Au(111) Surface. *ACS Nano* **2018**, *12* (7), 6452−6457.

(5) Goh, K. S.; Jimenez-Ruiz, M.; Johnson, M. R.; Rols, S.; Ollivier, J.; Denning, M. S.; Mamone, S.; Levitt, M. H.; Lei, X.; Li, Y.; Turro, N. J.; Murata, Y.; Horsewill, A. J. Symmetry-breaking in the endofullerene H_2O@C60 revealed in the quantum dynamics of ortho and para-water: a neutron scattering investigation. *Phys. Chem. Chem. Phys.* **2014**, *16* (39), 21330−9.

(6) Kurotobi, K.; Murata, Y. A Single Molecule of Water Encapsulated in Fullerene C60. *Science* **2011**, *333*, 613−616.

(7) Zhukova, E. S.; Torgashev, V. I.; Gorshunov, B. P.; Lebedev, V. V.; Shakurov, G. S.; Kremer, R. K.; Pestrjakov, E. V.; Thomas, V. G.; Fursenko, D. A.; Prokhorov, A. S.; Dressel, M. Vibrational states of a water molecule in a nano-cavity of beryl crystal lattice. *J. Chem. Phys.* **2014**, *140* (22), 224317.

(8) Gorshunov, B. P.; Torgashev, V. I.; Zhukova, E. S.; Thomas, V. G.; Belyanchikov, M. A.; Kadlec, C.; Kadlec, F.; Savinov, M.; Ostapchuk, T.; Petzelt, J.; Prokleska, J.; Tomas, P. V.; Pestrjakov, E. V.; Fursenko, D. A.; Shakurov, G. S.; Prokhorov, A. S.; Gorelik, V. S.; Kadyrov, L. S.; Uskov, V. V.; Kremer, R. K.; Dressel, M. Incipient ferroelectricity of water molecules confined to nano-channels of beryl. *Nat. Commun.* **2016**, *7*, 12842.

(9) Dong, A.-N.; Sun, L.-H.; Tang, X.-Q.; Yao, Y.-K.; An, Y.; Hao, D.; Shan, X.-Y.; Lu, X.-H. Observation of Simplest Water Chains on Surface Stabilized by a Hydroxyl Group at One End. *Chin. Phys. Lett.* **2019**, *36* (11), 116801.

(10) Peng, J.; Guo, J.; Hapala, P.; Cao, D.; Ma, R.; Cheng, B.; Xu, L.; Ondracek, M.; Jelinek, P.; Wang, E.; Jiang, Y. Weakly perturbative imaging of interfacial water with submolecular resolution by atomic force microscopy. *Nat. Commun.* **2018**, *9* (1), 122.

(11) Shiotari, A.; Sugimoto, Y. Ultrahigh-resolution imaging of water networks by atomic force microscopy. *Nat. Commun.* **2017**, *8*, 14313.

(12) Stipe, B. C.; Rezaei, M. A.; Ho, W. Single-Molecule Vibrational Spectroscopy and Microscopy. *Science* **1998**, *280*, 1732−1735.

(13) Kim, Y.; Komeda, T.; Kawai, M. Single-molecule reaction and characterization by vibrational excitation. *Phys. Rev. Lett.* **2002**, *89* (12), 126104.

(14) Li, S.; Yu, A.; Toledo, F.; Han, Z.; Wang, H.; He, H. Y.; Wu, R.; Ho, W. Rotational and vibrational excitations of a hydrogen molecule trapped within a nanocavity of tunable dimension. *Phys. Rev. Lett.* **2013**, *111* (14), 146102.

(15) Guo, J.; Lü, J.-T.; Feng, Y.; Chen, J.; Peng, J.; Lin, Z.; Meng, X.; Wang, Z.; Li, X.-Z.; Wang, E.-G.; Jiang, Y. Nuclear quantum effects ofhydrogen bonds probed by tip-enhanced inelastic electron tunneling. *Science* **2016**, *352* (6283), 321−325.

(16) Vitali, L.; Ohmann, R.; Kern, K.; Garcia-Lekue, A.; Frederiksen, T.; Sanchez-Portal, D.; Arnau, A. Surveying molecular vibrations during the formation of metal-molecule nanocontacts. *Nano Lett.* **2010**, *10* (2), 657−60.
(17) Choi, T.; Ruggiero, C. D.; Gupta, J. A. Incommensurability and atomic structure of c(2 × 2)N/Cu(100): A scanning tunneling microscopy study. *Phys. Rev. B: Condens. Matter Mater. Phys.* **2008**, *78* (3), 035430.
(18) Driver, S. M.; Hoeft, J.-T.; Polcik, M.; Kittel, M.; Terborg, R.; Toomes, R. L.; Kang, J.-H.; Woodruff, D. P. Cu(100)c(2 × 2)-N: a new type of adsorbate-induced surface reconstruction. *J. Phys.: Condens. Matter* **2001**, *13*, L601−L606.
(19) Ruggiero, C. D.; Badal, M.; Choi, T.; Gohlke, D.; Stroud, D.; Gupta, J. A. Emergence of surface states in nanoscale Cu_2N islands. *Phys. Rev. B: Condens. Matter Mater. Phys.* **2011**, *83* (24), 245430.
(20) Guo, J.; Meng, X.; Chen, J.; Peng, J.; Sheng, J.; Li, X. Z.; Xu, L.; Shi, J. R.; Wang, E.; Jiang, Y. Real-space imaging of interfacial water with submolecular resolution. *Nat. Mater.* **2014**, *13* (2), 184−9.
(21) Nishino, T.; Hayashi, N.; Bui, P. T. Direct measurement of electron transfer through a hydrogen bond between single molecules. *J. Am. Chem. Soc.* **2013**, *135* (12), 4592−5.
(22) Nishino, T.; Ito, T.; Umezawa, Y. A fullerene molecular tip can detect localized and rectified electron tunneling within a single fullerene−porphyrin pair. *Proc. Natl. Acad. Sci. U. S. A.* **2005**, *102*, 5659−5662.
(23) Verlhac, B.; Bachellier, N.; Garnier, L.; Ormaza, M.; Abufager, P.; Robles, R.; Bocquet, M.-L.; Ternes, M.; Lorente, N.; Limot, L. Atomic-scale spin sensing with a single molecule at the apex of a scanning tunneling microscope. *Science* **2019**, *366*, 623−627.
(24) Martinez, J. I.; Abad, E.; Gonzalez, C.; Flores, F.; Ortega, J. Improvement of scanning tunneling microscopy resolution with H-sensitized tips. *Phys. Rev. Lett.* **2012**, *108* (24), 246102.
(25) Klimeš, J.; Bowler, D. R.; Michaelides, A. Van der Waals density functionals applied to solids. *Phys. Rev. B: Condens. Matter Mater. Phys.* **2011**, *83* (19), 195131.
(26) Kresse, G.; Joubert, D. From ultrasoft pseudopotentials to the projector augmented-wave method. *Phys. Rev. B: Condens. Matter Mater. Phys.* **1999**, *59*, 1758−1775.
(27) King, G. W.; Hainer, R. M.; Cross, P. C. The Asymmetric Rotor I. Calculation and Symmetry Classification of Energy Levels. *J. Chem. Phys.* **1943**, *11* (1), 27−42.
(28) Wang, S. C. On the Asymmetrical Top in Quantum Mechanics. *Phys. Rev.* **1929**, *34* (2), 243−252.
(29) Tennyson, J.; Bernath, P. F.; Brown, L. R.; Campargue, A.; Császár, A. G.; Daumont, L.; Gamache, R. R.; Hodges, J. T.; Naumenko, O. V.; Polyansky, O. L.; Rothman, L. S.; Vandaele, A. C.; Zobov, N. F.; Al Derzi, A. R.; Fábri, C.; Fazliev, A. Z.; Furtenbacher, T.; Gordon, I. E.; Lodi, L.; Mizus, I. I. IUPAC critical evaluation of the rotational−vibrational spectra of water vapor, Part III: Energy levels and transition wavenumbers for $H_2{}^{16}O$. *J. Quant. Spectrosc. Radiat. Transfer* **2013**, *117*, 29−58.
(30) Polyansky, O. L.; Ovsyannikov, R. I.; Kyuberis, A. A.; Lodi, L.; Tennyson, J.; Zobov, N. F. Calculation of rotation-vibration energy levels of the water molecule with near-experimental accuracy based on an ab initio potential energy surface. *J. Phys. Chem. A* **2013**, *117* (39), 9633−43.
(31) Gorshunov, B. P.; Zhukova, E. S.; Torgashev, V. I.; Lebedev, V. V.; Shakurov, G. S.; Kremer, R. K.; Pestrjakov, E. V.; Thomas, V. G.; Fursenko, D. A.; Dressel, M. Quantum Behavior of Water Molecules Confined to Nanocavities in Gemstones. *J. Phys. Chem. Lett.* **2013**, *4* (12), 2015−20.

https://dx.doi.org/10.1021/acs.jpclett.0c00093
J. Phys. Chem. Lett. 2020, 11, 1650−1655